White Rose Research Online

eprints@whiterose.ac.uk
https://eprints.whiterose.ac.uk
Universities of Leeds, Sheffield and York

Deposited via The University of Sheffield.

White Rose Research Online URL for this paper:
https://eprints.whiterose.ac.uk/id/eprint/245995/

Version: Published Version

**Article:**
Crowther, P.A. and Smith, E.L. (2026) Detection of new Galactic Wolf-Rayet stars with SPHEREx. Monthly Notices of the Royal Astronomical Society. stag1822. ISSN: 0035-8711

https://doi.org/10.1093/mnras/stag1822

**Reuse**
This article is distributed under the terms of the Creative Commons Attribution (CC BY) licence. This licence allows you to distribute, remix, tweak, and build upon the work, even commercially, as long as you credit the authors for the original work. More information and the full terms of the licence here: https://creativecommons.org/licenses/

**Takedown**
If you consider content in White Rose Research Online to be in breach of UK law, please notify us by emailing eprints@whiterose.ac.uk including the URL of the record and the reason for the withdrawal request.

UNIVERSITY OF LEEDS
University of Sheffield
UNIVERSITY of York

# Detection of new Galactic Wolf-Rayet stars with SPHEREx

Paul A. Crowther[1]★, Erin L. Smith[1]
[1]*Astrophysics Research Cluster, School of Mathematical and Physical Sciences, University of Sheffield, Hicks Building, Hounsfield Road, Sheffield S3 7RH, UK*

Accepted XXX. Received YYY; in original form ZZZ

**ABSTRACT**

We assess the potential for the NASA Explorer SPHEREx mission in adding to the Milky Way census of Wolf-Rayet (WR) stars by extracting 0.75–5$\mu$m spectrophotometry of 30 candidate WR stars previously identified using *Gaia* XP spectra. We confirm an additional Galactic 13 WR (8 WN and 5 WC) stars, identify 3 probable [WC]-type central stars of Planetary Nebulae, plus 2 He emission line sources. SPHEREx has the potential to detect additional relatively isolated WR stars on the far size of the Milky Way by combining Machine Learning techniques with a judicious choice of candidate selection criteria. Indeed SPHEREx is sufficiently sensitive to identify bright Magellanic Cloud Wolf-Rayet stars.

**Key words:** stars: Wolf-Rayet – stars: emission-line – infrared: stars – Galaxy: stellar content – planetary nebulae: general

## 1 INTRODUCTION

Classical Wolf-Rayet (WR) stars are evolved descendents of massive OB-type stars, possess dense, fast outflows and so exhibit unusually strong, broad emission lines across the electromagnetic spectrum (Shenar 2026). Their strong winds often dictate the fate of massive stars (Romagnolo et al. 2024). Very massive stars (VMS) also resemble WR stars owing to their proximity to the Eddington limit (Crowther et al. 2010). Consequently, WR stars and VMS represent useful tracers of recent star-formation in galaxies, and provide sources of mechanical, radiative and chemical feedback in young populations (Crowther 2007). A subset of H-depleted planetary nebulae central stars also exhibit similar spectral morphologies (Todt & Hamann 2015; Weidmann et al. 2020).

Historically, Galactic WR stars were primarily detected serendipitously via H$\alpha$ surveys (e.g. Hopewell et al. 2005) or dedicated optical narrow-band surveys (Shara et al. 1999). Since they are primarily located in the dusty thin-disk of the Milky Way, detected sources are generally confined to the Solar Neighbourhood, such that the Galactic WR census stood at 227 a quarter of a century ago (van der Hucht 2001). Fortunately, the advent of efficient large format infrared detectors over the last couple of decades has permitted searches for Wolf-Rayet stars and other emission line sources within the entire Galactic plane (Crowther 2015). To date, approximately 700 Wolf-Rayet stars have been identified in the Milky Way[1], yet the total has been estimated to lie between 1500 (Shara et al. 1999) and 6500 (van der Hucht 2001).

In particular, since the infrared colours of Wolf-Rayet stars are unusual, owing to free-free emission from their dense stellar winds, candidates have been identified from colour-colour diagrams (Hadfield et al. 2007; Mauerhan et al. 2011; Faherty et al. 2014), combining Two Micron All Sky Survey (2MASS, Skrutskie et al. 2006a) with *Spitzer*/GLIMPSE (Benjamin et al. 2003) or *WISE* (Wright et al. 2010) observations of the Galactic plane. In parallel, Shara et al. (2009, 2012) used several narrow $K_s$-band filters – sensitive to specific WR emission lines – to image the Galactic plane using ground-based telescopes, resulting in complementary Wolf-Rayet candidates. Nevertheless, such searches are relatively inefficient since WR stars are rare, and contaminants are common (e.g. Hadfield et al. 2007; Rosslowe & Crowther 2018). Rich, dust-obscured, young star clusters have also been successfully targeted (Crowther et al. 2006a; Davies et al. 2012; Chené et al. 2013).

The bulk of available infrared WR spectra is restricted to the JHK windows between 1–2.5$\mu$m (Figer et al. 1997; Crowther et al. 2006a; Nishimaki et al. 2008; Shara et al. 2012), although spectroscopy beyond 2.5$\mu$m has been obtained with the SpeX instrument at the *Infra Red Telescope Facility* (Faherty et al. 2014), plus various space-based telescopes, including the Short-Wavelength Spectrometer (SWS) aboard *Infrared Space Observatory* (van der Hucht et al. 1996; Dessart et al. 2000; Morris et al. 2000), the Infrared Spectrograph (IRS) on *Spitzer* (Morris et al. 2004; Ignace et al. 2007), Photodetector Array Camera and Spectrometer (PACS) aboard *Herschel* (Crowther et al. 2024), plus the Mid Infrared Instrument (MIRI) on *JWST* (Lau et al. 2022).

In this study we combine Spectro-Photometer for the History of the Universe, Epoch of Reionization, and Ices Explorer (SPHEREx, Bock et al. 2026) with candidate WR stars identified from a Machine Learning analysis (Creevey et al. 2023) of low-resolution *Gaia* BP/GP (hereafter XP) spectroscopy (De Angeli et al. 2023). A subset of such WR candidates have been confirmed via follow-up optical spectroscopy (Marin et al. 2024; Mulato et al. 2025), but many additional candidates exist, representing test cases for the capabilities of SPHEREx for Milky Way emission line stars. Machine learning techniques sometimes identify emission line sources with some spectroscopic similarities to WR stars, albeit with a very different nature such as Cataclysmic Variables (e.g. SW Sex, Chang et al. 2025). *Gaia* XP candidates and SPHEREx are introduced in Section 2, low resolution spectroscopy of WR stars and related sources are presented in Section 3, new candidates are discussed in Section 4, with brief discussion and conclusions drawn in Section 5.

★ E-mail: Paul.Crowther@sheffield.ac.uk

[1] v1.35 of the online catalogue maintained at http://pacrowther.staff.shef.ac.uk/WRcat

© The Author(s) 2026. Published by Oxford University Press on behalf of Royal Astronomical Society. This is an Open Access article distributed under the terms of the Creative Commons Attribution License (https://creativecommons.org/licenses/by/4.0/), which permits unrestricted reuse, distribution, and reproduction in any medium, provided the original work is properly cited.

ORIGINAL UNEDITED MANUSCRIPT

Downloaded from academic.oup.com/mnras/advance-article/doi/10.1093/mnras/stag1822/8836705 by guest on 28 September 2026

**Table 1.** Low resolution (SL, 5.2–14.5$\mu$m) *Spitzer*/IRS datasets of WR stars and related emission line sources used in the present study, including AOR (Astronomical Observation Request) number. *Spitzer*/IRS datasets of WR1 and WR52 have previously been discussed by Ignace et al. (2007).

| Star | Sp Type | Obs | AOR | PI (programme) |
|---|---|---|---|---|
| WR1 | WN4b | Oct 2004 | 10440704 | Leitherer (3185) |
| WR52 | WC4 | Mar 2006 | 14237440 | Crowther (20154) |
| WR142 | WO2 | Jun 2005 | 12414464 | Houck (199) |
| NGC 6905 | [WO1] | Jun 2007 | 21969152 | Fazio (40115) |
| NGC 40 | [WC8] | Nov 2007 | 21976832 | Fazio (40115) |
| M4-18 | [WC10] | Nov 2008 | 21957632 | Bernard-Salas (40035) |
| He 3-519 | early B Ia$^+$ | May 2005 | 13735680 | Calibration |

## 2 SPECTROPHOTOMETRY

### 2.1 SPHEREx

SPHEREx (Bock et al. 2026) is a NASA Explorer mission undertaking an all-sky survey across 102 narrow-bands between 0.75–5$\mu$m, corresponding to a resolving power of $R$ = 35-41 ($\leq$ 3.8$\mu$m, Bands B1-B4), $R$ = 110 (3.8-4.4$\mu$m, Band B5) or $R$ = 130 (4.4-5.0$\mu$m, Band B6) at a coarse spatial resolution (6.2″ pixels). SPHEREx was launched on 11 March 2025, commenced regular science operations on 1 May 2025 and is due to complete 4 observations of the sky in each filter position over its nominal 2 year operation. The SPHEREx data processing pipeline is described in Akeson et al. (2025). The SPHEREx Spectrophotometry Tool[2] provides forced photometry of point sources for each narrow-band image, with a choice of background region, defaulting to 15 pixels, using `the Tractor`[3]. Calculation of the background incorporates catalogued IR point sources, or these can be manually added when undertaking spectrophotometry of targets. Observations discussed here were processed in July 2026, so generally represent two observations per filter position.

In principle, the experimental design of SPHEREx is well suited to the identification of heavily reddened WR stars owing to their rich emission line spectra and their predicted peak $K_s$-band magnitude of ~10 (Rosslowe & Crowther 2015), which corresponds to $F_\nu$ = 65 mJy. Indeed, the majority of all Galactic WR stars are anticipated to be brighter than $K_s$ = 15 mag or $F_\nu$ = 0.65 mJy (Rosslowe & Crowther 2015, their figure 12) for which solely strong emission lines would readily be detected. In addition, the brightest WR stars at IR wavelengths may suffer from saturation effects. In summary, SPHEREx covers a similar spectral range to *JWST* NIRSpec/PRISM (Böker et al. 2023), albeit with a somewhat lower resolving power, and is suited to milli-Jy rather than nano-Jy sources.

### 2.2 *Spitzer*/IRS

Although the primary focus of this study is SPHEREx, a subset of Wolf-Rayet stars and related emission line objects have been observed with the Infrared Spectrograph (IRS) aboard *Spitzer* (Houck et al. 2004). The bluest module (Short-Low, SL) of IRS covered the 5.2–14.5$\mu$m range at a resolving power of ~100, in first (7.6–14.5$\mu$m, SL1) or second (5.2–7.6$\mu$m, SL2) order, with a 2 pixel slit width corresponding to 3.6″.

Therefore, *Spitzer*/IRS provides spectral coverage of WR stars adjacent to SPHEREx at a comparable resolving power. Previous studies of WR stars using *Spitzer*/IRS have included Morris et al. (2004) and Ignace et al. (2007), which primarily focused on mid-IR fine structure lines. Archival SL *Spitzer*/IRS spectroscopy retrieved from the *Spitzer* Heritage Archive were reduced using the final version (v18.18) of the pipeline[4]. Table 1 provides details of IRS spectroscopy presented in this study, including Astronomical Observation Request (AOR) numbers, since some targets have multiple observations in the archive. All datasets used were acquired in Stare (as opposed to Map) mode.

### 2.3 Emission line stars from *Gaia* XP

Beyond its astrometric capabilities, *Gaia* also provides medium resolution spectroscopy of visually bright sources around the calcium triplet (RVS, Cropper et al. 2018), plus low resolution XP spectrophotometry for sources with $G$ < 19 mag (De Angeli et al. 2023). The latter XP dataset was released in Data Release 3, covering the wavelength ranges 0.33-0.68 $\mu$m (BP, $R$=30-100) and 0.64-1.05$\mu$m (RP, $R$=70-100), and correspond to cut-outs of 3.5×2.1 arcsec$^2$ (Carrasco et al. 2021). Creevey et al. (2023) introduce a Machine Learning approach in which the Extended Stellar Parametrizer for Emission Line Stars (ESP-ELS) module assigns probabilities for Be, Herbig Ae/Be, T Tauri, active M dwarfs, Planetary Nebulae (PNe) or Wolf-Rayet stars based on their *Gaia* XP spectra. Mulato et al. (2026) discuss candidate PNe from ESP-ELS.

Amongst the 565 Wolf-Rayet candidates from ESP-ELS, half have an assigned `classlabel_espels_flag` of 0 (very high probability), with the remainder spread between flags 1 (high probability) to 4 (low probability). The overwhelming majority of sources with a 0 flag are previously known Milky Way or Magellanic Cloud WR stars. Mulato et al. (2025) identified 59 candidate WR stars from ESP-ELS, utilising IR broad-band colour criteria of Mauerhan et al. (2011). Of these, the brightest 37 candidates were observed spectroscopically, with 33 sources confirmed - three of which were in common with Marin et al. (2024). We shall investigate the nature of the remaining high probability ESP-ELS candidate WR stars. All candidates discussed, with the exception of the Planetary Nebula NGC 6751 and candidate [WC]-type star G326.5-0.6, have *Gaia* re-normalised unit weight error (RUWE) values below the 1.25 threshold recommended to exclude unresolved binaries (Penoyre et al. 2022).

## 3 SPHEREX OBSERVATIONS OF WR STARS AND RELATED OBJECTS

### 3.1 Wolf-Rayet stars

Representative spectrophotometry of (mostly) Galactic Wolf-Rayet stars from SPHEREx are presented in Fig. 1, including archival *Spitzer*/IRS low-resolution spectroscopy, where available, which extend to Pf$\alpha$ (Sect. 2.2). Owing to the low resolving power of SPHEREx, we have also consulted unpublished *IRTF*/SpeX observations of Galactic WR stars (W.D. Vacca, priv. comm.), which helped establish the near-IR classification scheme for WR stars of Rosslowe & Crowther (2018).

The upper panel compares the strong-lined early WN star WR1 (HD 4004, black) to the late WN star WR123 (HD 177230, red), including a zoomed in view of the critical 1$\mu$m region in the top right subpanel. The most prominent emission lines in WR1 are

[2] https://irsa.ipac.caltech.edu/applications/spherex/tool-spectrophotometry
[3] http://github.com/dstndstn/tractor
[4] https://www.ipac.caltech.edu/doi/irsa/10.26131/IRSA399

ORIGINAL UNEDITED MANUSCRIPT

Downloaded from academic.oup.com/mnras/advance-article/doi/10.1093/mnras/stag1822/8836705 by guest on 28 September 2026

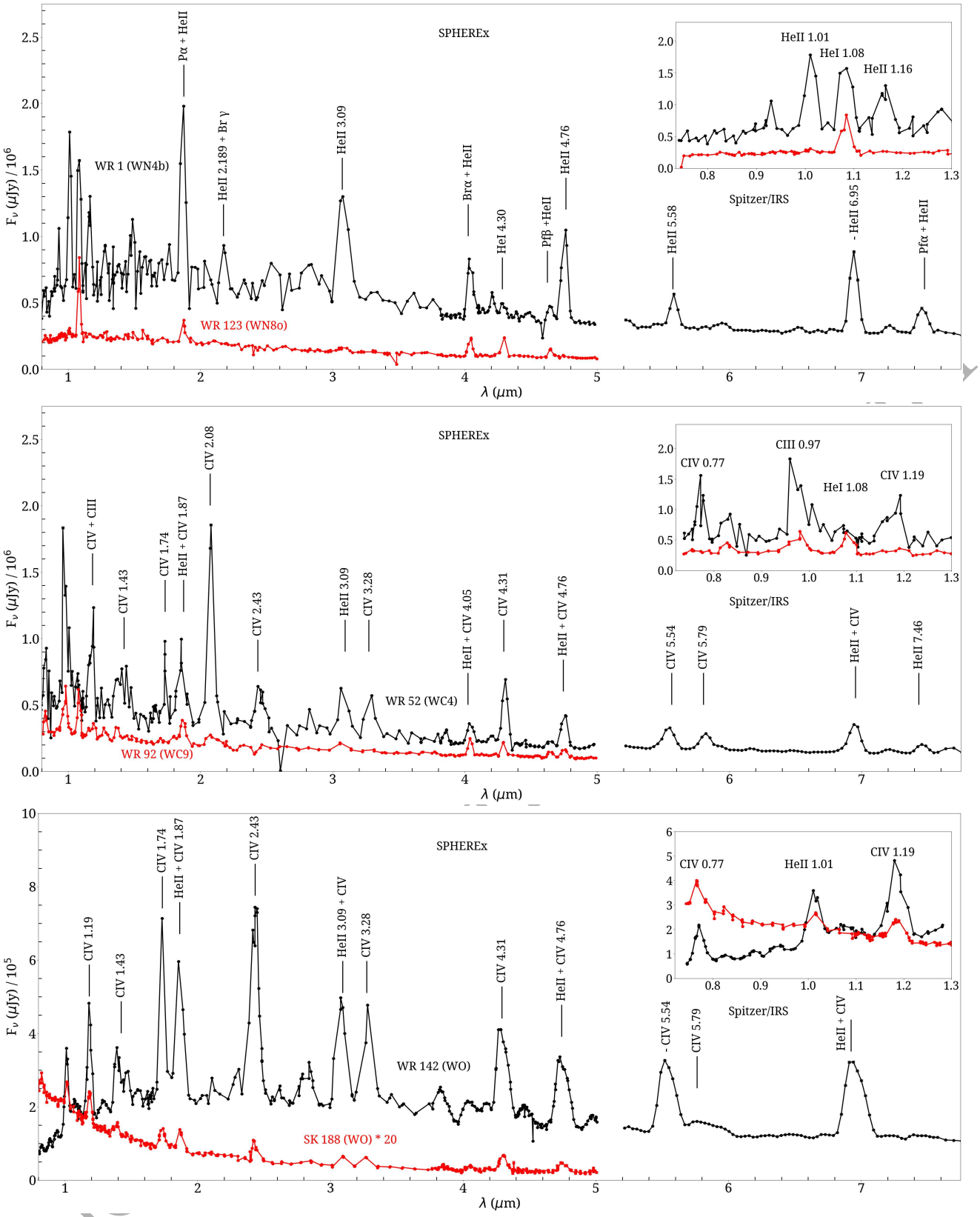



**Figure 1.** SPHEREx spectrophotometry of representative WN stars WR1 (black) and WR123 (red) in the upper panel, WC stars WR52 (black) and WR92 (red) in the middle panel and the WO stars WR142 (black) and Sk 188 (red, SMC star whose flux has been scaled by factor of 20) in the lower panel. Low resolution (SL) *Spitzer*/IRS spectroscopy of WR1, WR52 and WR142 is included, with zoomed in spectra around 1$\mu$m shown in the upper right side of each panel.

Downloaded from academic.oup.com/mnras/advance-article/doi/10.1093/mnras/stag1822/8836705 by guest on 28 September 2026

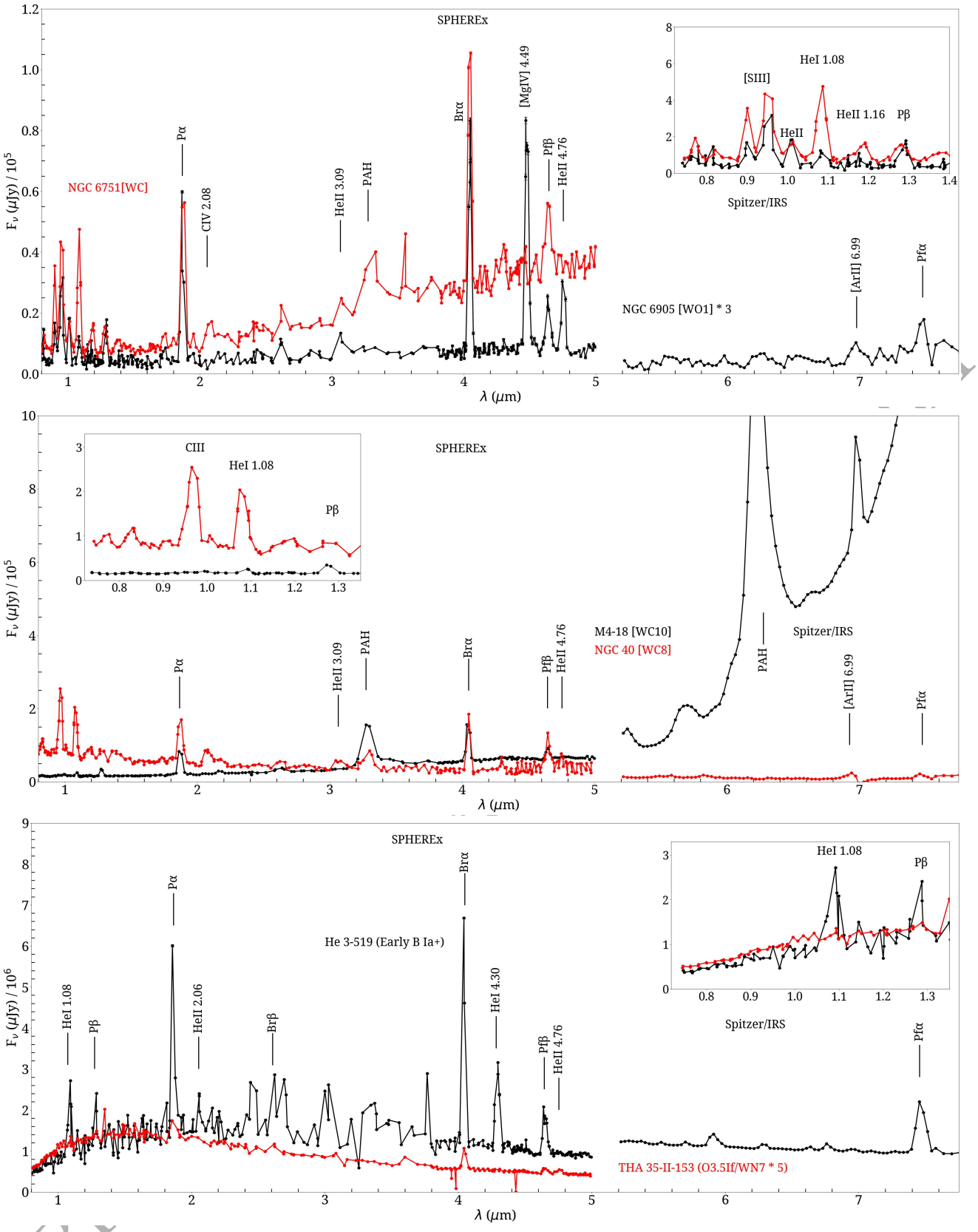



**Figure 2.** SPHEREx spectrophotometry of high excitation Wolf-Rayet type CSPNe NGC 6905 (black, [WO]) and NGC 6751 (red, [WC4]) in the upper panel, low excitation CSPNe M4-18 [(black, [WC10]) and NGC 40 (red, [WC8]) in the middle panel and extreme OB supergiants He 3–519 (early B supergiant, black) and THA 35-II-153 (O3.5 If/WN7, red) in the lower panel. Low resolution (SL) *Spitzer*/IRS spectroscopy of NGC 6905, M4-18, NGC 40 and He 3–519 is included, revealing strong PAH emission at 6.2$\mu$m in M4-18, with zoomed in spectra around 1$\mu$m shown in each panel. The flux of NGC 6905 has been scaled by a factor of 3 and THA 35-II-153 (WR31-1) has been scaled by a factor of 5 for clarity.

Downloaded from academic.oup.com/mnras/advance-article/doi/10.1093/mnras/stag1822/8836705 by guest on 28 September 2026

He II 1.01$\mu$m (5–4), 1.86$\mu$m (6–5), 3.09$\mu$m (7–6), 4.76$\mu$m (8-7), 6.95$\mu$m (9-8, *Spitzer*/IRS), plus He I 1.08$\mu$m. WR 1 is hydrogen-free (Hamann et al. 2006), so leading hydrogen lines are produced by corresponding He II lines, such as He II (10-8) instead of Br$\alpha$ (5–4). Unusually for late WN stars, WR123 is also highly deficient in hydrogen (Massey & Conti 1980; Crowther et al. 1995), and since He II lines are weakly present in late WN stars, He I components of (4–3) and (5–4) transitions will dominate the prominent P$\alpha$ and Br$\alpha$ features (Morris et al. 2000) as well as He I 1.08$\mu$m and 4.30$\mu$m. Weaker near-IR He I lines at 1.70$\mu$m and 2.06$\mu$m are difficult to identify with SPHEREx.

The middle panel of Fig. 1 compares the early WC star WR52 (HD 115473, black) to the WC9 star WR92 (HD 157451, red). The most prominent emission lines in WR52 are C IV 2.08$\mu$m, followed by C IV $\alpha$ transitions, including 1.19$\mu$m (8–7), 1.74$\mu$m (9–8), 2.43$\mu$m (10–9), 3.28$\mu$m (11–10), 4.31$\mu$m (12–11), 5.54$\mu$m (13–12, *Spitzer*/IRS), plus C III 0.97$\mu$m and He II 1.01$\mu$m, 3.09$\mu$m, 4.76$\mu$m. The high ionization features are less pronounced in the WC9 star, with C III 0.97$\mu$m and He I 1.08$\mu$m amongst the most prominent features (see zoomed in view in the subpanel).

The lower panel of Fig. 1 shows the WO stars WR142 (Sand 5, black) and Sk 188 (AB8, SMC, red) whose IR spectra are dominated by most of the same C IV emission lines as WR52, with the exception of 2.08$\mu$m which is suppressed in WO stars (see Tramper et al. 2015), plus corresponding He II transitions, with He I absent. C IV 0.77$\mu$m and 1.19$\mu$m are clearly observed in WO stars (see zoomed in subpanel), aided by the high wind velocities of WO stars (Kingsburgh et al. 1995). The SMC WO binary is relatively faint ($K_S$ = 13.3 mag) so its flux has been scaled by a factor of 20. Indeed, Sk 188 (WO+O4, Moffat et al. 1985) is one of numerous Magellanic Cloud WR systems to be readily detected with SPHEREx.

Emission lines in dusty WC stars will often be masked by hot dust (Williams 2019), except at the bluest SPHEREx wavelengths (I, Y and J bands), and the low spectral resolution will hinder the detection of weak emission lines, such as He II 1.01$\mu$m, 3.09$\mu$m in late WN stars (e.g. WR123 in Fig. 1). The coarse spatial resolution of SPHEREx may also lead to severe dilution of WR emission lines by nearby IR continuum sources. This can be assessed by comparison with higher spatial resolution ($\sim 2''$) photometry from 2MASS (Skrutskie et al. 2006a) and/or the GLIMPSE survey using *Spitzer*/IRAC (Benjamin et al. 2003). *WISE* W1 (3.5$\mu$m) and W2 (4.6$\mu$m) band observations provide a superior sky coverage to GLIMPSE (Wright et al. 2010), albeit at comparable spatial resolution to SPHEREx.

### 3.2 Ionized nebulae

The low resolving power of SPHEREx generally prevents strong nebular emission lines (tens of km s$^{-1}$) being easily distinguished from Wolf-Rayet emission lines (thousands of km s$^{-1}$), since $R \sim 40$ for Bands B1 to B4 corresponds to FWHM$\sim$ 7500 km s$^{-1}$. Exceptions include WO stars (e.g. WR142 in Fig. 1) and broad spectral lines in the highest resolution Band B6 for which FWHM$\sim$ 2300 km s$^{-1}$. H II regions will generally exhibit strong nebular P $\alpha$, Br $\alpha$ and He I emission in the SPHEREx wavelength range, together with [S III] 0.91+0.95$\mu$m, but their ionizing sources are insufficient hard to produce nebular He II 1.01, 1.86, 3.09 or 4.76$\mu$m, and often show broad 3.3$\mu$m PAH emission in their associated photo dissociation regions (PDRs, Verstraete et al. 2001).

In contrast, the ionizing stars of Planetary Nebulae (PNe) are capable of producing nebular He II in addition to H I, He I, plus forbidden [S III] 0.91+0.95$\mu$m as well as [Mg IV] 4.49$\mu$m (Bernard Salas et al. 2001), so the presence of collisionally excited forbidden lines helps PNe to be distinguished from WR stars. By way of example, Fig. A1 includes SPHEREx spectrophotometry of the planetary nebula NGC 2392 whose central star (CSPN) is a subdwarf O star (Pauldrach et al. 2004; Kudritzki et al. 2006).

PNe with [WC] or [WO]-type central stars are more problematic regarding the potential for confusion with WC and WO stars, since they also produce stellar He II and C IV emission. To illustrate their similarities, the upper panel of Fig. 2 presents SPHEREx spectrophotometry of high excitation CSPNe, NGC 6905 and NGC 6751, which have [WO1] and [WC4] spectral types, respectively (Crowther et al. 1998), together with *Spitzer*/IRS spectroscopy of NGC 6905. C IV 2.08$\mu$m is observed in NGC 6751, while other leading stellar C IV recombination lines (e.g. 1.74$\mu$m) are present in both sources, suggesting a mix of stellar and nebular origin for He II 1.01$\mu$m, 1.86$\mu$m, 3.09$\mu$m, 4.76$\mu$m emission. Both exhibit nebular [S III] 0.91+0.95$\mu$m (see zoomed in subpanel), plus [Mg IV] 4.49$\mu$m is observed in NGC 6905.

The middle panel of Fig. 2 presents SPHEREx spectrophotometry of low excitation CSPNe, M4-18 and NGC 40, which have [WC10] (De Marco & Crowther 1999) and [WC8] (Crowther et al. 1998) spectral types, respectively, together with *Spitzer*/IRS spectroscopy. M4-18 is dominated by nebular emission, including [Ar II] 6.99$\mu$m plus strong PAH emission (6.2$\mu$m, 3.3$\mu$m), plus Paschen and Brackett lines and He I 1.08$\mu$m (see zoomed in subpanel). NGC 40 emission includes nebular Paschen and Brackett lines, plus stellar wind lines (e.g. C III 0.97$\mu$m in subpanel) from the [WC 8] central star, so would be difficult to distinguish from WC stars solely from IR spectroscopy.

### 3.3 OB supergiants

It has been established for several decades that early-type supergiants exhibit IR emission lines (McGregor et al. 1988; Hanson et al. 1996; Mauerhan et al. 2010; Clark et al. 2012). In particular, very strong H I and He I emission lines are observed in B hypergiants such as P Cygni (Najarro et al. 1997), HDE 316285 (Hillier et al. 1998) and He 3-519 (Smith et al. 1994), but they are too cool to produce He II emission that would be detectable with SPHEREx. Potential stellar He II emission line sources are O supergiants (Hanson et al. 1996; Morris et al. 1996; Bohannan & Crowther 1999), albeit with weaker signatures than late-type WN stars (Lenorzer et al. 2002, see their fig. 7).

The lower panel of Fig. 2 presents SPHEREx spectrophotometry of two close relatives of classical WR stars – He 3–519 (early B Ia$^+$) and THA 35-II-153 (O3.5 If*/WN7, Maíz Apellániz et al. 2016) – indeed both have WR catalogue aliases WR31a and WR31-1, respectively. THA 35-II-153 reveals weak He II 4.76$\mu$m emission (1.01$\mu$m is not detected - see subpanel). *Spitzer*/IRS spectroscopy of He 3–519 is included, revealing strong Pf$\alpha$ emission, with a modest flux offset between SPHEREx and *Spitzer*/IRS spectroscopy, likely arising from the associated ejecta nebula (Smith et al. 1994).

## 4 SPHEREX OBSERVATIONS OF WR CANDIDATES

Table 2 provides an overview of WR candidates discussed in this section, including *Gaia* DR3 identifications, aliases from Mulato et al. (2025), optical/IR photometry, and inferred absolute magnitudes in the J-band using distances from Bailer-Jones et al. (2021) inferred from *Gaia* parallaxes. The J-band is favoured over the $K_s$-band in this instance since the $K_s$-band can be strongly affected by hot dust in the case of WC or [WC]-type stars (Crowther et al.

ORIGINAL UNEDITED MANUSCRIPT

Downloaded from academic.oup.com/mnras/advance-article/doi/10.1093/mnras/stag1822/8836705 by guest on 28 September 2026

2006b; Williams 2019) despite the higher uncertainties in J-band extinctions. Adopted Bayesian priors affect parallax-inferred distances, as discussed by Rate & Crowther (2020), but we adhere to those from Bailer-Jones et al. (2021) since our targets likely include a mixture of evolved massive and lower mass stars. Extinctions for non-dusty WR stars, $A_J$, are estimated using intrinsic JHK colours from Rosslowe & Crowther (2015) and $A_J/A_K = 2.5$ (Indebetouw et al. 2005), and are presented in Table 2. In the case of dusty WC stars, since $JHK_s$ colours are contaminated by hot dust – identified from 2MASS plus *Spitzer*/GLIMPSE (Benjamin et al. 2003) or *WISE* (Wright et al. 2010) mid-IR photometry, such that *Gaia* $G_{BP} - G_{RP}$ colours are preferred to estimate $A_J$ following Rate & Crowther (2020, their figure 9). For WR70-19 a parallax-based distance is not known, so this is estimated from weak-lined WN5-6 absolute J-band magnitudes (Rate & Crowther 2020).

ORIGINAL UNEDITED MANUSCRIPT

Downloaded from academic.oup.com/mnras/advance-article/doi/10.1093/mnras/stag1822/8836705 by guest on 28 September 2026

**Table 2.** Newly confirmed Galactic Wolf-Rayet stars and related emission line sources from SPHEREx spectrophotometry obtained from *Gaia* ESP-ELS candidates (Creevey et al. 2023), including the numerical value of `classlabel_espels_flag`, ranging from 0 (very high probability) to 4 (low probability). Aliases from Mulato et al. (2025, MMC25) are included. Photometry is from *Gaia* ($G_{BP}$, $G_{RP}$), 2MASS ($JHK_s$) and *WISE* (W1). Photogeometric distance moduli (DM) are inferred from *Gaia* DR3 parallax (Bailer-Jones et al. 2021), while $A_J$ follows Rosslowe & Crowther (2015), aside from dusty WC stars for which *Gaia* observed $G_{BP} - G_{RP}$ colours are used to estimate $A_J \sim 2.5A_K$ (Rate & Crowther 2020). J-band absolute magnitudes, $M_J$, are generally inferred from J, $A_J$ and DM (→) with the exception of WR70-19 for which DM is inferred from J, $A_J$, and an adopted $M_J$ (←) from Rate & Crowther (2020).

| ID | ESP-ELS | *Gaia* DR3 | MMC25 | RA | Dec | *l* | *b* | $G_{BP}$ | $G_{RP}$ | J | H | $K_s$ | W1 | DM | $A_J$ | | $M_J$ | SpT | Notes |
|---|---|---|---|---|---|---|---|---|---|---|---|---|---|---|---|---|---|---|---|
| | | | | — J2000 — | | deg | deg | mag | mag | mag | mag | mag | mag | mag | mag | | mag | | |
| **New Wolf-Rayet stars** | | | | | | | | | | | | | | | | | | | |
| WR44-2 | 0 | 5333920438969809152 | WR-C-08 | 11:24:36.53 | –62:32:35.0 | 293.1101 | –1.3388 | 19.42 | 15.27 | 11.95 | 10.71 | 9.85 | 8.94 | $13.1^{+0.7}_{-0.6}$ | $2.0^{+0.2}_{-0.2}$ | → | $-3.1^{+0.7}_{-0.6}$ | WN4-6b | ··· |
| WR62-3 | 0 | 5878372204454901248 | WR-C-15 | 14:35:08.70 | –61:14:02.5 | 315.0793 | –0.8323 | 19.32 | 15.45 | 12.68 | 11.81 | 11.25 | 10.58 | $13.8^{+0.6}_{-0.6}$ | $2.0^{+0.2}_{-0.2}$ | → | $-3.1^{+0.6}_{-0.6}$ | WN3 | ··· |
| WR70-18 | 0 | 5882603507496595200 | WR-C-19 | 15:37:41.30 | –57:23:35.8 | 323.8861 | –1.4482 | 17.99 | 14.94 | 12.80 | 11.99 | 11.18 | 10.44 | $14.4^{+0.6}_{-0.4}$ | $1.5^{+0.2}_{-0.2}$ | → | $-3.1^{+0.6}_{-0.4}$ | WC7–8 | ··· |
| WR70-19 | 1 | 5884578986303334016 | ··· | 15:55:08.61 | –54:59:20.7 | 327.2791 | –1.0483 | 16.97 | 14.25 | 12.01: | 11.27 | 10.74 | 9.57 | $13.8^{+0.7}_{-0.7}$ | $2.0^{+0.7}_{-0.7}$ | ← | $-3.8^{+0.7}_{-0.7}$ | WN6–7 | ··· |
| WR77-9 | 0 | 5939996017261315968 | WR-C-22 | 16:49:41.87 | –46:45:08.7 | 339.1529 | –1.3322 | 19.76 | 14.71 | 11.27 | 10.06 | 9.13 | 8.12 | $13.3^{+0.7}_{-0.6}$ | $3.0^{+0.3}_{-0.3}$ | → | $-5.0^{+0.7}_{-0.6}$ | WC9d | ··· |
| WR84-13 | 1 | 5971904330062036224 | WR-C-25 | 17:14:00.39 | –40:30:42.1 | 346.7762 | -0.9822 | 19.80 | 15.72 | 12.60 | 11.39 | 10.33 | 9.13 | $13.1^{+1.0}_{-0.6}$ | $2.5^{+0.2}_{-0.2}$ | → | $-3.0^{+1.0}_{-0.6}$ | WC9d | ··· |
| WR84-14 | 0 | 5965760637051514496 | ··· | 17:14:24.11 | –41:57:25.1 | 345.6467 | –1.8873 | 17.45 | 14.70 | 12.27: | 11.33 | 10.81 | 10.24 | $13.8^{+0.3}_{-0.6}$ | $1.5^{+0.2}_{-0.2}$ | → | $-3.0^{+0.4}_{-0.6}$ | WN7 | ··· |
| WR94-5 | 1 | 4054402569982187904 | WR-C-27 | 17:33:23.11 | –33:43:52.5 | 354.5509 | –0.3424 | 18.20 | 14.68 | 12.02 | 11.23 | 10.66 | 10.01 | $13.6^{+0.4}_{-0.3}$ | $1.4^{+0.2}_{-0.2}$ | → | $-3.0^{+0.5}_{-0.4}$ | WN6 | ··· |
| WR98-3 | 2 | 4056935402389532672 | WR-C-30 | 17:41:27.51 | –30:16:42.6 | 358.3827 | +0.0654 | 20.50 | 14.83 | 10.27 | 7.93 | 6.10 | 3.61 | $13.5^{+0.6}_{-0.7}$ | $3.2^{+0.3}_{-0.3}$ | → | $-6.4^{+0.6}_{-0.7}$ | WC9d | ··· |
| WR111-16 | 0 | 4066281766676330368 | WR-C-33 | 18:08:52.12 | –23:55:27.1 | 6.9458 | –1.9871 | 19.02 | 14.70 | 11.56 | 10.24 | 9.04 | 7.91 | $13.6^{+0.6}_{-0.6}$ | $2.8^{+0.3}_{-0.3}$ | → | $-4.8^{+0.6}_{-0.6}$ | WC4–7d | ··· |
| WR125-7 | 1 | 2021131933611057536 | WR-C-51 | 19:38:34.47 | +24:03:20.5 | 59.5413 | +1.1401 | 19.76 | 16.23 | 13.56 | 12.66 | 11.99 | 11.02 | $14.3^{+0.5}_{-0.5}$ | $1.7^{+0.2}_{-0.2}$ | → | $-2.5^{+0.5}_{-0.5}$ | WN5–6 | ··· |
| WR128-1 | 1 | 1828324426391283200 | WR-C-52 | 19:52:40.81 | +23:29:33.9 | 60.6724 | –1.9343 | 18.03 | 15.26 | 13.32 | 12.56 | 12.01 | 11.05 | $14.1^{+0.4}_{-0.7}$ | $1.5^{+0.2}_{-0.2}$ | → | $-2.3^{+0.4}_{-0.7}$ | WN4–5 | ··· |
| WR148-3 | 1 | 2169491477039398144 | WR-C-56 | 21:05:28.26 | +51:36:00.8 | 91.6922 | +2.9904 | 19.73 | 15.82 | 12.91 | 11.84 | 11.06 | 10.19 | $14.2^{+0.5}_{-0.9}$ | $1.8^{+0.2}_{-0.2}$ | → | $-3.1^{+0.5}_{-0.9}$ | WN4b | ··· |
| **New Wolf-Rayet CSPNe** | | | | | | | | | | | | | | | | | | | |
| G307.2-0.6 | 0 | 5865253866850321280 | WR-C-13 | 13:29:11.16 | –63:10:09.2 | 307.1763 | –0.6090 | 19.75 | 15.64 | 12.72 | 11.67 | 10.74: | 10.01 | $12.7^{+0.3}_{-0.3}$ | $1.9^{+0.2}_{-0.2}$ | → | $-1.9^{+0.4}_{-0.4}$ | [WC8–9] | ··· |
| G326.5-0.6 | 1 | 5884420446123080320 | WR-C-20 | 15:48:50.49 | –55:11:20.2 | 326.4534 | –0.6345 | 18.98 | 14.31 | 10.54 | 8.52 | 6.94 | 5.57 | $8.9^{+0.2}_{-0.2}$ | $2.7^{+0.3}_{-0.3}$ | → | $-1.1^{+0.4}_{-0.4}$ | [WC9] | ··· |
| G31.2-1.3 | 0 | 4258982586850246784 | WR-C-45 | 18:53:05.40 | –02:08:33.2 | 31.2130 | –1.3442 | 19.55 | 15.78 | 13.29 | 12.45 | 11.56 | 10.97 | $12.7^{+0.5}_{-0.7}$ | $1.7^{+0.2}_{-0.2}$ | → | $-1.1^{+0.5}_{-0.7}$ | [WC7–8] | ··· |
| **Other emission-line sources** | | | | | | | | | | | | | | | | | | | |
| PMR 1 | 4 | 5313911079687293440 | ··· | 09:28:40.97 | –49:36:46.6 | 272.8387 | +1.0325 | 17.75 | 16.03 | 14.19 | 13.56 | 13.15 | 12.38 | $11.8^{+0.4}_{-0.4}$ | $0.8^{+0.2}_{-0.2}$ | → | $+1.6^{+0.4}_{-0.4}$ | [WC] | ··· |
| ··· | 2 | 5258760366715078656 | WR-C-06 | 10:15:21.03 | –57:07:05.9 | 282.9434 | –0.4324 | 16.83 | 14.00 | 11.67 | 10.32 | 8.83 | 6.91 | $13.5^{+0.2}_{-0.2}$ | $4.1^{+0.8}_{-0.8}$ | → | $-5.9^{+0.8}_{-0.8}$ | ··· | He I em. |
| WR85a | 0 | 5973474703218558080 | ··· | 17:16:02.18 | –38:15:42.7 | 348.8328 | +0.0110 | 13.88 | 11.60 | 9.71 | 8.43 | 6.83 | 4.84 | $12.5^{+0.1}_{-0.1}$ | $4.3^{+1.0}_{-1.0}$ | → | $-7.1^{+1.0}_{-1.0}$ | ··· | He I em. |
| ··· | 3 | 4095106941425872640 | WR-C-34 | 18:09:48.33 | –19:18:00.7 | 11.0988 | +0.0594 | 18.49 | 15.35 | 12.47 | 10.80 | 9.38 | 7.61 | $12.4^{+0.3}_{-0.2}$ | $3.8^{+0.3}_{-0.3}$ | → | $-3.7^{+0.4}_{-0.4}$ | WC? | C III em. |
| J1823+0250 | 2 | 4277897038692284032 | ··· | 18:23:47.04 | +02:50:17.5 | 32.3107 | +7.4450 | 16.17 | 15.19 | 14.60 | 14.41 | 14.33 | ··· | $13.9^{+0.3}_{-0.4}$ | $0.8^{+0.2}_{-0.2}$ | → | $-0.1^{+0.4}_{-0.4}$ | WN-like | He II em |
| NGC 6751 | 3 | 4206136209740612352 | ··· | 19:05:55.54 | –05:59:32.9 | 29.2275 | –5.9418 | 13.61 | 13.81 | 13.37 | 13.23 | 12.63 | 10.02 | $12.5^{+0.3}_{-0.3}$ | $0.1^{+0.1}_{-0.1}$ | → | $+0.8^{+0.4}_{-0.4}$ | [WC] | ··· |
| J1907-0523 | 3 | 4206279695997383040 | ··· | 19:07:39.60 | –05:23:33.3 | 29.9613 | –6.0570 | 16.74 | 16.07 | 15.33 | 15.26 | 15.27 | 14.55 | $14.3^{+0.4}_{-0.4}$ | $0.6^{+0.1}_{-0.1}$ | → | $+0.4^{+0.4}_{-0.4}$ | WN-like | He II em |
| ··· | 2 | 2059241178412827520 | WR-C-53 | 20:09:08.72 | +36:38:00.9 | 73.7111 | +1.9795 | 17.74 | 15.66 | 14.50 | 13.92 | 13.39 | 11.66 | $14.2^{+0.3}_{-0.5}$ | $1.7^{+0.2}_{-0.2}$ | → | $-1.4^{+0.4}_{-0.5}$ | WN? | He II em? |

ORIGINAL UNEDITED MANUSCRIPT

Downloaded from academic.oup.com/mnras/advance-article/doi/10.1093/mnras/stag1822/8836705 by guest on 28 September 2026

### 4.1 High probability candidates

We have extracted SPHEREx spectrophotometry of Wolf-Rayet candidates with `classlabel_espels_flag` in the range 0 to 2, excluding: (i) known WR stars; (ii) other stellar types (e.g. Young Stellar Objects, Cataclysmic Variables); (iii) candidates spectroscopically observed by Mulato et al. (2025); (iv) sources at high galactic latitude i.e. $|b| \geq 10°$; (v) peculiar emission line sources (e.g. HD 45166, WR85a). HD 45166 has historically been described as a quasi-WR star, but Shenar et al. (2023) firmly established it as a highly magnetic He star, resulting from a merger. Low resolution optical spectroscopy of WR85a closely resembles the unusual He-rich, nebular dominated source WR122 (Crowther & Smith 1999; Mauerhan et al. 2015). WR85a is known to exhibit He I 1.08$\mu$m emission (Morris et al. 1996), although its nature remains uncertain.

13 of the 22 remaining candidates are confirmed as Wolf-Rayet stars – 8 WN and 5 WC stars – which are presented in Fig. 3 and Fig. 4, respectively. Photometry from 2MASS (open circles, Skrutskie et al. 2006b), *Spitzer*/GLIMPSE (open squares, Benjamin et al. 2003), and *WISE* (open triangles, Wright et al. 2010) is included. SPHEREx spectrophotometry generally matches photometry, with the exception of *WISE* photometry of WR44-2. Assigned WR catalogue numbers follow the 2012 IAU Working Group for Massive Star recommendations presented in Appendix A of Rosslowe & Crowther (2015), i.e. WR44-2 denotes the second identified Galactic WR whose Right Ascension lies between WR44 and WR45 (van der Hucht 2001).

The low resolution SPHEREx spectrophotometry hinders IR spectral classification (Rosslowe & Crowther 2018), due to line blends (e.g. He I 1.70$\mu$m/He II 1.69$\mu$m, C III 1.20$\mu$m/C IV 1.19$\mu$m) and distinguishing narrow-lined from broad-lined WN stars. Nevertheless, estimates of the emission equivalent width of He II 1.01$\mu$m permits strong-lined early WN stars to be distinguished from weak-lined early WN stars (Smith et al. 1996), and the He I 1.08$\mu$m/He II 1.01$\mu$m ratio (recall insets in Fig. 1) permits spectral type estimates (Rosslowe & Crowther 2018). Since emission lines may be diluted by other IR sources in the vicinity of the WR star, the SPHEREx band (B6) with the highest resolving power includes He II 4.76$\mu$m. WR136 narrowly qualifies as a strong, broad-lined WN star (WNb) with FWHM(He II 4.76$\mu$m) $\sim$ 2500 km s$^{-1}$, uncorrected for instrumental broadening, below which WN stars are classified as weak, narrow-lined.

From the spectrophotometry presented in Figure 3 we identify WR44-2 and WR148-3 as strong-lined (WNb) early-type stars, with WR62-3, WR70-20, WR84-14, WR94-5, WR128-1 and WR125-7 as weak-lined stars, ranging from WN3 (WR62-3) to WN7 (WR84-14).

For WC stars, the relative strengths of C III 0.97$\mu$m, He II 1.01$\mu$m and He I 1.08$\mu$m provide the primary diagnostics (recall insets in Fig. 1), since the ratio of C IV 2.08$\mu$m to C III 2.11$\mu$m recommended by Rosslowe & Crowther (2018) is severely hindered by the low resolution of SPHEREx band B3. From the spectrophotometry presented in Figure 4 we identify WR111-16 as a WC4–7, WR70-18 as a WC7–8 star since C III $\gg$ He I $\gtrsim$ He II, plus WR77-9, WR84-13 and WR98-3 as WC9 stars owing to C III $\sim$ He I $\gg$ He II. Rising flux levels from $K_s$-band to GLIMPSE [3.6] or *WISE* W1 3.5$\mu$m suggest the presence of hot dust (WC $\rightarrow$ WCd), with WR98-3 the most obvious example in Fig. 4.

Turning to the remaining ESP-ELS Wolf-Rayet candidates, three systems match those of WC stars albeit with unrealistically faint absolute magnitudes. SPHEREx spectrophotometry of these sources is presented in the Appendix (Fig. A1), together with the Planetary Nebula NGC 2392, an early [WC]-type central star PMR 1 (Morgan et al. 2001) plus a late WC star. WR-C-20 (Mulato et al. 2025) resembles a WC9 star, though has a suspiciously low distance (0.6 kpc). This has remained undetected to date owing to its very high dust extinction, as evidenced by its very red *Gaia* colour $G_{BP} - G_{RP}$ = 4.67 mag. Examples of nearby, highly reddened WR systems exist e.g. WR70-16 (Apep, Callingham et al. 2019, 2020). Nevertheless, the absolute J-band magnitude of WR-C-20, $M_J$ = –1.1±0.4 mag, is over three magnitudes fainter than typical WC9 stars (Rate & Crowther 2020), so we favour a [WC]-type CSPNe origin, and subsequently refer to it by its galactic coordinates G326.5–0.6, adding to the catalogue of low-galactic latitude [WC] stars (Kanarek et al. 2017).

A coarse estimate of the bolometric luminosity of G326.5–0.6 can be made from comparison with Potsdam WR (PoWR) model atmosphere (Gräfener et al. 2002; Hamann & Gräfener 2003) grids of WC stars (Sander et al. 2012). The Galactic WC 06-12 model[5], with properties appropriate to WC9 stars (Rate & Crowther 2020), has $BC_J$ = –3.6 mag, so the estimated luminosity for G326.5–0.6 is $\log L/L_\odot \sim 3.8$, typical of CSPNe (Bloecker 1995; Miller Bertolami 2016). We have also estimated absolute J-band magnitudes of well known CSPNe NGC 40 [WC8] and BD+30° 3639 [WC9] using distances and $c(H\beta)$ from Bucciarelli & Stanghellini (2023). Each have $M_J \sim +0.5$ mag using 2MASS photometry of their central stars. Similar arguments apply to the more distant, also late-type, [WC] sources WR-C-13 (G307.2–0.6) and WR-C-45 (G31.2–1.3) from Mulato et al. (2025). We marginally favour a massive star nature for WR84-13 (WC9d) despite its modest absolute J-band magnitude owing to its location in the thin-disk ($z$ = 70 pc) and its estimated bolometric luminosity ($\log L/L_\odot \sim 4.5$) exceeds that of luminous post-AGB stars (Bloecker 1995).

Of the *Gaia* ESP-ELS candidates observed by Mulato et al. (2025), WR-C-06 reveals emission at He I 1.08$\mu$m and P$\alpha$, although there is no evidence for He II emission, in agreement with. their conclusions that this is not a WR star. Several additional candidates remain viable WR stars on the basis of their spectrophotometry with SPHEREx, including the candidate WN star WR-C-53 for which He II 1.01$\mu$m, 4.76$\mu$m are detected with low significance.

Another candidate which will be denoted by its RA/Dec coordinates (J1823+0250) is confirmed as a (weak) He emission line star, including He II 1.01$\mu$m, 1.86$\mu$m, 3.09$\mu$m, 4.76$\mu$m, plus He I 1.08$\mu$m (see Fig. A2 in the Appendix). We estimate its J-band extinction from its $G_{BP} - G_{RP}$ *Gaia* colour (Rate & Crowther 2020), indicating an absolute J-band magnitude of $M_J = -0.1^{+0.4}_{-0.4}$ mag, several magnitudes fainter than WN stars (Rate & Crowther 2020), and its *Gaia* parallax infers a large distance from the galactic plane ($|z| = 0.78^{+0.16}_{-0.12}$ kpc). Consequently J1823+0250 is a potential intermediate mass (stripped) Helium star, for which Götberg et al. (2018) solar metallicity He star models with 4.5 to 5.1 $M_\odot$ infer absolute J-band magnitudes of +0.3 and –0.45 mag, respectively. Indeed, absolute J-band magnitudes of stripped He stars in the Magellanic Clouds (Drout et al. 2023; Götberg et al. 2023) range from –1.0 mag (star 1, star 5) to +0.9 mag (star 4) on the basis of VMC photometry (Cioni et al. 2011).

Intermediate mass stripped He stars are generally expected to possess weak winds (Sander & Vink 2020). J1823+0250 merits further study since it may correspond to a transition spectrum between a dominant WR-like emission at high mass, and subdwarf O-type absorption at low mass (Götberg et al. 2018, their figure 5). In general the low resolving power hinders an assessment of whether He II emission is stellar or nebular, but the higher resolving power of SPHEREx Band B6 is consistent either with a nebular origin of He II 4.76$\mu$m, or a slow wind if it is stellar in origin, indicating of a hot, He-rich source in either case.

[5] https://www.astro.physik.uni-potsdam.de/PoWR/powrgrid1.php

ORIGINAL UNEDITED MANUSCRIPT

Downloaded from academic.oup.com/mnras/advance-article/doi/10.1093/mnras/stag1822/8836705 by guest on 28 September 2026

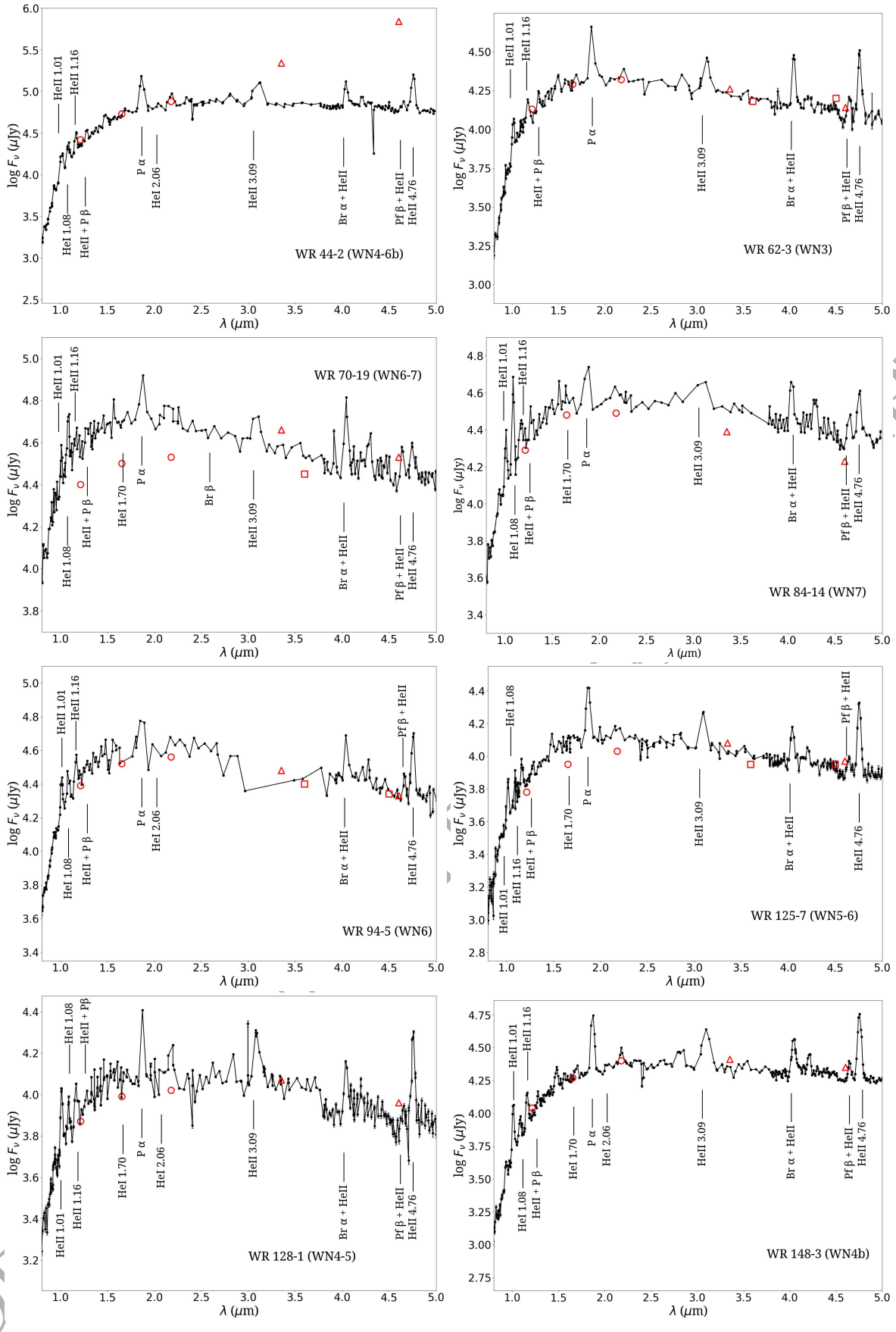



**Figure 3.** SPHEREx spectrophotometry of newly identified WN stars, together with photometry from 2MASS (open circles), *Spitzer*/GLIMPSE (open squares) and *WISE* (open triangles). Fluxes are in logarithmic units given the wide dynamic range of spectrophotometry.

Downloaded from academic.oup.com/mnras/advance-article/doi/10.1093/mnras/stag1822/8836705 by guest on 28 September 2026

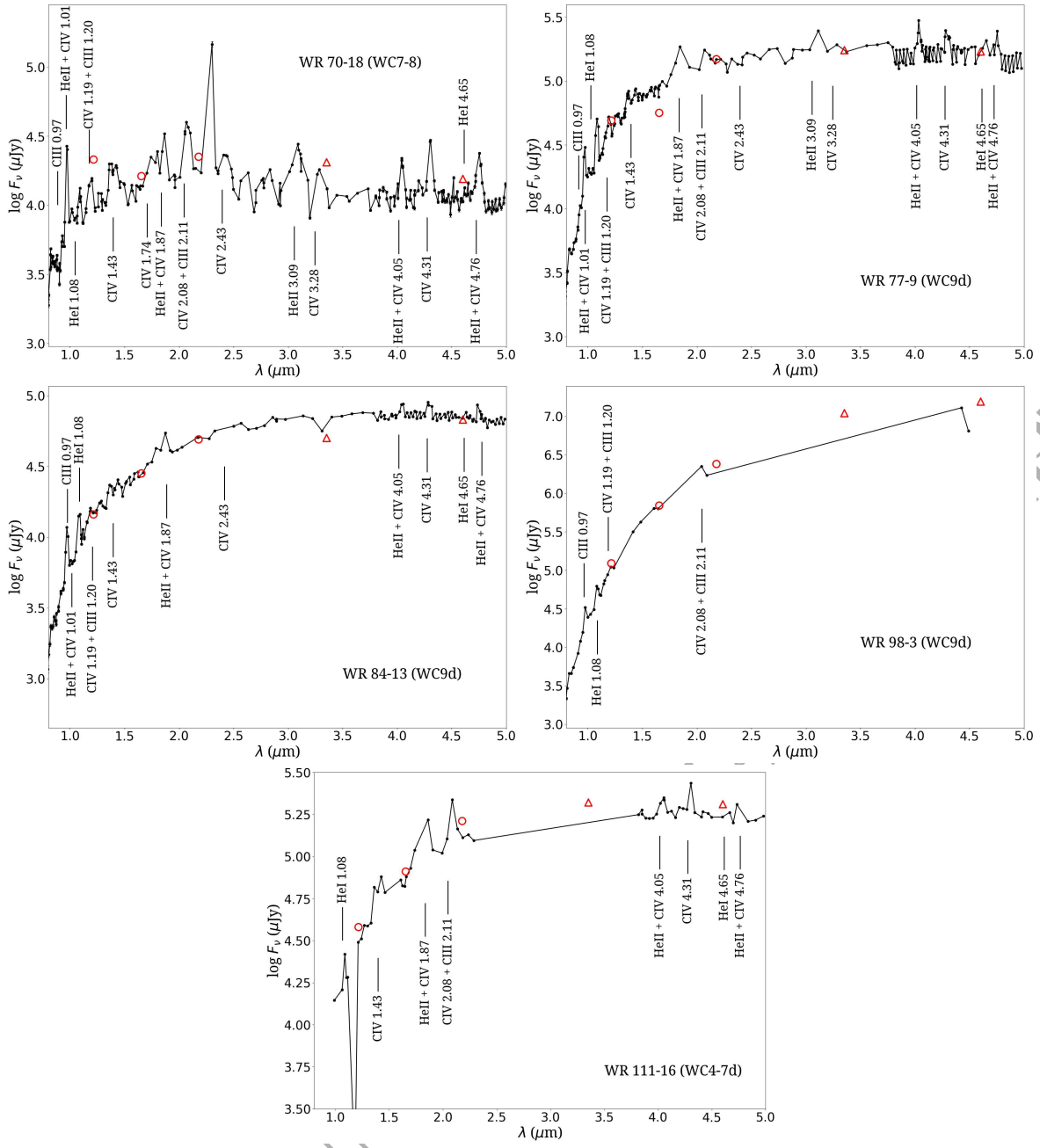



**Figure 4.** SPHEREx spectrophotometry of newly identified WC stars, together with photometry from 2MASS (open circles) and *WISE* (open triangles). Fluxes are in logarithmic units given the wide dynamic range of spectrophotometry.

Sources with spectroscopic similarities to WR stars in the visual include Cataclysmic Variables (CVs) - indeed Chang et al. (2025) attributed a spectrum of the CV SW Sex from LAMOST DR10 to a WN star. Excluding any foreground J-band extinction, the absolute J-band magnitude of SW Sex is +5.3 mag based on its *Gaia* DR3 parallax-derived distance of 0.60 kpc (Bailer-Jones et al. 2021), so one can exclude such an origin for J1823+0250.

Müller-Horn et al. (2026) have recently identified a WN star in a close binary system, WR2-1, from SDSS-V Milky Way Mapper (MWM) spectroscopy (Kollmeier et al. 2026). Strong emission-lines from the WN star are heavily diluted by the brighter O star companion at visual wavelengths, which may explain why it eluded detection from previous H$\alpha$ surveys. WR2-1 has a systemic absolute magnitude of $M_J = -4.1^{+0.2}_{-0.2}$ mag assuming a *Gaia* DR3 photogeometric distance of $6.45^{+0.56}_{-0.66}$ kpc (Bailer-Jones et al. 2021). Adopting the extinction of $A_V = 5.5$ mag ($A_J = 1.5$ mag) and the 25±5% contribution of the WR star to the J-band flux from Müller-Horn et al. (2026), its absolute J-band magnitude is $-2.4^{+0.3}_{-0.3}$ mag, comparable to many newly identified WN stars from this study. SPHEREx spectroscopy of WR2-1 is included in the Appendix (Fig. A2), with He II 3.09$\mu$m, 4.76$\mu$m emission lines observed, plus P$\alpha$+He II and Br$\alpha$+He II. He II 1.01$\mu$m is not observed, presumably owing to the greater contribution from the O star companion at shorter wavelengths, He II 4.76$\mu$m has a modest FWHM owing to the slow wind of its WN component.

ORIGINAL

Downloaded from academic.oup.com/mnras/advance-article/doi/10.1093/mnras/stag1822/8836705 by guest on 28 September 2026

**Table 3.** Overview of key stellar and nebular emission line diagnostics observed in the SPHEREx wavelength range for WNE, WNL, WCE/WO (and [WCE]/[WO]), WCL (and [WCL]), Planetary Nebulae (PNe), O and B supergiants. Parenthesis indicate weak feature.

| $\lambda$ ($\mu$m) | Ion | WNE | WNL | WCE/ WO | WCL | PNe | O | B supergiant |
|---|---|---|---|---|---|---|---|---|
| 0.77 | C IV 7-6 | – | – | ✓ | – | – | – | – |
| 0.95 | [S III] | – | – | – | – | ✓ | – | – |
| 0.97 | C III 3d-3p | – | | (✓) | ✓ | – | – | – |
| 1.01 | He II 5-4+C IV 10-8 | ✓ | (✓) | ✓ | (✓) | (✓) | (✓) | – |
| 1.08 | He I 2p-2s | (✓) | ✓ | (✓) | ✓ | ✓ | (✓) | ✓ |
| 1.19 | C IV 8-7 | – | – | ✓ | – | – | – | – |
| 1.28 | P$\beta$ | (✓) | (✓) | – | – | ✓ | – | (✓) |
| 1.74 | C IV 9-8 | – | – | ✓ | – | – | – | – |
| 1.87 | P$\alpha$+He II 6-5 | ✓ | ✓ | ✓ | (✓) | ✓ | (✓) | ✓ |
| 2.06 | He I 2p-2s | – | (✓) | – | (✓) | – | – | (✓) |
| 2.08 | C IV 3d-3p | – | – | ✓ | (✓) | – | – | – |
| 2.43 | C IV 10-9 | – | – | ✓ | – | – | – | – |
| 2.62 | Br$\beta$ | (✓) | (✓) | – | – | ✓ | – | (✓) |
| 3.09 | He II 7-6+C IV 14-12 | ✓ | (✓) | ✓ | (✓) | (✓) | (✓) | – |
| 3.28 | C IV 11-10 | – | – | ✓ | – | – | – | – |
| 4.05 | Br$\alpha$+He II 10-8 | ✓ | ✓ | ✓ | (✓) | ✓ | (✓) | ✓ |
| 4.30 | C IV 12-11+He I 3p-3s | (✓) | ✓ | ✓ | (✓) | – | – | ✓ |
| 4.49 | [Mg IV] | – | – | – | – | ✓ | – | – |
| 4.65 | Pf$\beta$ | (✓) | (✓) | – | – | ✓ | – | (✓) |
| 4.76 | He II 8-7+C IV 16-14 | ✓ | (✓) | ✓ | (✓) | (✓) | (✓) | – |

### 4.2 Low probability candidates

We have extracted SPHEREx observations for 8 additional ESP-ELS candidate WR stars with `classlabel_espels_flag` = 3 or 4. Most candidates are at relatively high Galactic latitude so are unlikely to be genuine Milky Way WR stars, so we focus solely on sources with $|b| \leq 10°$. These include WR-C-34 (Mulato et al. 2025) which remains a viable WC candidate since C III 0.97$\mu$m is detected, but the spectrum is unusable at longer wavelengths. WR-C-04 exhibits strong P$\alpha$ and Br$\alpha$ emission, although lacks any evidence for He I-II emission. Br$\alpha$, Pf$\beta$ emission is also observed in WR-C-02, while the only prominent spectral feature in WR-C-07 is 3.3$\mu$m PAH emission. The lack of He II emission in WR-C-02, WR-C-04 or WR-C-07 agrees with the non-WR identification of these sources by Mulato et al. (2025).

Another He emission line star amongst the ESP-ELS candidates is J1907-0523, whose SPHEREx spectral morphology is consistent with an early-type, weak-lined WN star (Fig. A2). However, a massive star origin for J1907-0523 is excluded (as for J1823+0250) owing to its modest absolute J-band magnitude of $M_J = +0.4^{+0.4}_{-0.4}$ mag on the basis of a *Gaia* DR3 photogeometric distance of $7.1^{+1.6}_{-1.4}$ kpc (Bailer-Jones et al. 2021), and $A_J$ estimated from its *Gaia* $G_{BP} - G_{RP}$ colour. This source also lies at a large distance from the mid-plane ($|z| = 0.75^{+0.15}_{-0.15}$ kpc), and matches the predicted J-band absolute magnitude of a ~$4M_\odot$ stripped He star model (Götberg et al. 2018). In contrast with J1823+0250, the higher resolving power of SPHEREx in Band B6 is indicative of a stellar origin of He II 4.76$\mu$m. Consequently, it is a second potential intermediate mass He star, so merits further study. Alternatively, it might be belong to the rare subset of PNe with [WN]-type central stars (e.g. IC 4663 Miszalski et al. 2012), but J1907-0523 lacks the strong nebular emission usually characteristic of PNe (NGC 2392 in Fig. A1).

Three low probability WR candidates at high Galactic latitude are

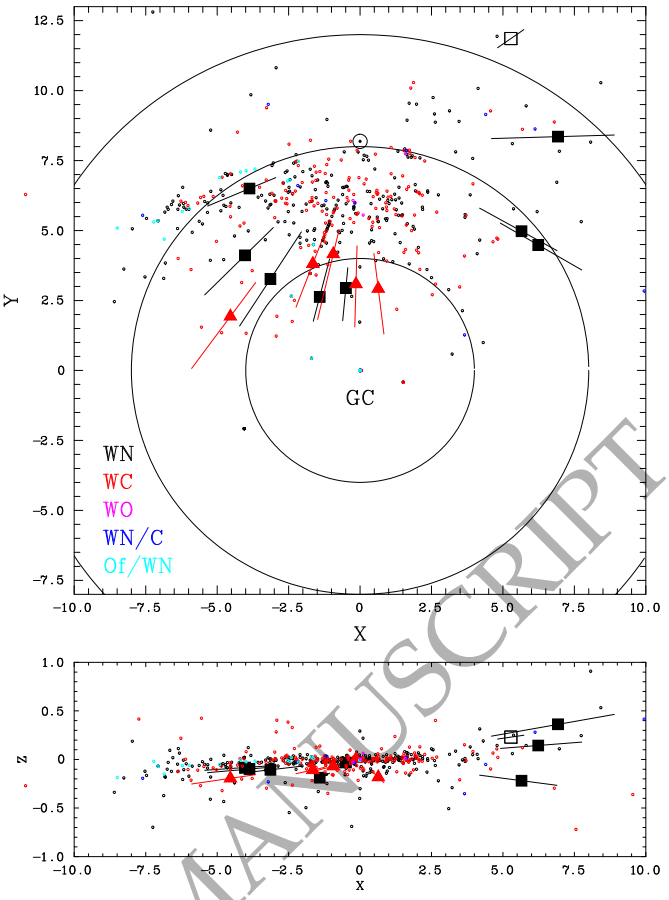



**Figure 5.** Location of newly identified WR stars - black squares for WN stars, red triangles for WC stars - together with estimated distances to previously known WR stars (open circles, key indicates subtypes) on a top down ($X, Y$) and side view ($X, Z$) of the Milky Way, in which the Galactic Centre is located at $X = Y = Z$=0 and the Sun is located at $X$=0, $Y$=8.15 kpc (Event Horizon Telescope Collaboration et al. 2022). Galactocentric distances of 4, 8 and 12 kpc are indicated, as is the recently identified O+WN system WR2-1 (open square Müller-Horn et al. 2026)

established [WC]-type PN central stars, NGC 6751 (Crowther et al. 1998), RaMul 2 (Werner et al. 2024) and PMR 1 (Morgan et al. 2001). Of these NGC 6751 and PMR 1 exhibit prominent emission lines in SPHEREx spectrophotometry, including broad 3.3$\mu$m PAH emission, while RaMul 2 is faint, with solely prominent C IV 2.08$\mu$m, 4.30$\mu$m emission. SPHEREx spectrophotometry for NGC 6751 is included in Fig. 2, with the [S III] 0.91+0.95$\mu$m doublet observed, while PMR 1 is presented in the Appendix (Fig. A1).

## 5 DISCUSSION AND CONCLUSIONS

Up until the advent of (very) large spectrophotometric datasets, courtesy of *Gaia* XP and SPHEREx, establishing the nature of Galactic emission line stars was a laborious, resource intensive undertaking. Candidates identified in photometric surveys, using narrow-band filters required dedicated spectroscopic follow-up at optical or IR wavelengths. Marin et al. (2024) and Mulato et al. (2025) have recently exploited the ESP-ELS analysis (Creevey et al. 2023) of *Gaia* XP spectrophotometry to confirm WR candidates using higher spectral resolution observations from ground-based facilities. High fore-

ORIGINAL UNEDITED MANUSCRIPT

Downloaded from academic.oup.com/mnras/advance-article/doi/10.1093/mnras/stag1822/8836705 by guest on 28 September 2026

ground dust extinction and the low resolving power hinders the use of *Gaia* XP in isolation since the primary spectral diagnostic (He II 0.469$\mu$m) lies in the blue visual.

We have used additional candidate Wolf-Rayet stars identified from ESP-ELS (Creevey et al. 2023) to illustrate the potential use of SPHEREx for the discovery of previously unknown WR and related stars, since useful diagnostics span the entire 0.75–5.0$\mu$m wavelength range. Care needs to be taken to exclude other emission line sources since the low resolving power of SPHEREx usually prevents strong nebular emission being distinguished from stellar emission. Table 3 provides an overview of key stellar and nebular emission lines observed in the SPHEREx wavelength range for WR, PNe and OB supergiants. Parentheses indicate weak emission features observed for each source type. SPHEREx is sufficiently sensitive that relatively isolated WR stars in the Magellanic Clouds can be easily identified, such as the WO binary Sk 188 in the SMC (Fig. 1).

Historical searches using He II 0.469$\mu$m emission and the adjacent continuum are sensitive to both WN and WC stars (Shara et al. 1999). Subsequent narrow-band IR photometric surveys conducted from ground-based facilities have generally focused on the $K_s$-band (Crowther et al. 2006a; Shara et al. 2009) in order to avoid high dust extinction at shorter wavelengths. Unfortunately, multiple filters are required in the $K_s$-band, since (most) WC stars exhibit strong C IV 2.08$\mu$m emission, while (most) WN stars show weaker emission in either He II 2.19$\mu$m or Br$\gamma$, such that Shara et al. (2009) adopted a six filter system. Since SPHEREx provides access to the full 0.75–5$\mu$m wavelength range, He II 3.09$\mu$m (mindful of potential PAH emission) or He II 4.76$\mu$m emission potentially provide spectral diagnostics of additional highly reddened WR stars, since only very late-type and dusty WR stars are weak in these lines.

Fig. 5 illustrates the location of the new WR stars within the Milky Way (top down, and side view), together with locations of all previously confirmed WR stars on the basis of distances from *Gaia* DR3 parallaxes (Rate & Crowther 2020; Bailer-Jones et al. 2021), the distance to the Galactic Centre (Event Horizon Telescope Collaboration et al. 2022) , distances to star clusters (Rate et al. 2020), or distance estimates from absolute magnitude calibrations (Rosslowe & Crowther 2015) otherwise. It is apparent that the newly reported WR stars are also on the near side of the Milky Way, with an average distance of 5.7±1.1 kpc. This is unsurprising since candidates are drawn from *Gaia* XP spectroscopy which is limited to sources brighter than $m_G$ = 19 mag. Most WR stars are close to the mid-plane, although some runaways are observed at surprisingly high vertical distances (Rate & Crowther 2020; Arthur 2025). The recently discovered O+WN system WR2-1 is indicated in Fig. 5 with a large open square.

Representative WR stars on the far side of the Milky Way, at galacto-centric distances of 4–8 kpc will lie 9–16 kpc away from the Sun (distance moduli 14.8 to 16.0), with a typical $K_s$-band dust extinction of $A_{K_s} \sim 1.5$ mag (higher in the direction of the Galactic Centre). Absolute $K_s$-band magnitudes of (non dusty) WR stars range from $M_{K_s}$ = –2 to –7 mag, but –5 mag is typical of mid WN and WC stars (Rosslowe & Crowther 2018), so anticipated $K_s$-band magnitudes are $11.3 \leq K_s \leq 12.5$ mag, well within the capabilities of SPHEREx.

Of course the faintest WR stars towards the dustiest sight-lines ($A_{K_s}$ = 3 mag), with $K_s \sim 17$ mag, would be challenging even neglecting the coarse spatial scale of SPHEREx. Distances to such objects would require infrared astrometry with the proposed *GaiaNIR* mission (Hobbs et al. 2021). Nevertheless, SPHEREx offers the prospect of increasing the known WR content of the Milky Way from targeted searches. All newly confirmed WR stars satisfy the primary IR photometric colour criteria of Faherty et al. (2014), as do most stellar dominated [WC]-type stars (the only exception is PMR 1).

In addition to searches for new WR stars, SPHEREx also permits previously reported WR stars to be verified. By way of example, the coordinates of the WN star 1603-75L (= WR123-4) from Shara et al. (2012) correspond to a non-2MASS source, yet they provide photometry for a 2MASS source 11 arcsec to the north with $K_s$=13.68 mag. SPHEREx spectrophotometry of WR123-4 shown in Fig. A1 confirms a late WC star at their quoted position, with $K_s \sim$12.4 mag.

In summary, we have presented a test application of SPHEREx for the discovery of Galactic WR stars, involving candidate WR stars using *Gaia* XP. Excluding recently confirmed candidates (Marin et al. 2024; Mulato et al. 2025), we confirm an additional 13 Milky Way WR stars, 8 WN and 5 WC, discuss similarities with [WC]-type CSPNe, and identify a few He emission line stars far from the galactic plane which may be intermediate mass He stars. The sensitivity of SPHEREx is capable of detecting WR stars on the far side of the Milky Way, indeed one example of a WR system in the SMC is presented. Consequently, SPHEREx has the potential to detect many more WR stars, by combining Machine Learning techniques with a judicious choice of candidate selection criteria.

## ACKNOWLEDGEMENTS

This research was made possible thanks to a Sheffield University Research Experience (SURE) summer placement for ELS. Thanks to Bill Vacca for providing the IRTF/SpeX datasets for a sample of Galactic Wolf-Rayet stars, and Lionel Mulato for sharing optical spectroscopy of a subset of ESP-ELS candidates. Thanks also to Ylva Götberg for helpful discussions regarding stripped Helium stars during the August 2026 Munich Institute for Astro-, Particle and BioPhysics (MIAPbP) workshop. MIAPbP is funded by the Deutsche Forschungsgemeinschaft (DFG, German Research Foundation) under Germany´s Excellence Strategy – EXC-2094 – 390783311. Comments from the anonymous referee helped clarify several aspects of the original manuscript.

This publication makes use of data products from the Spectro-Photometer for the History of the Universe, Epoch of Reionization and Ices Explorer (SPHEREx), which is a joint project of the Jet Propulsion Laboratory and the California Institute of Technology, and is funded by the National Aeronautics and Space Administration. This research has also made extensive use of the NASA/IPAC Infrared Science Archive, which is funded by the National Aeronautics and Space Administration and operated by the California Institute of Technology. This publication makes use of data products from the Wide-field Infrared Survey Explorer, which is a joint project of the University of California, Los Angeles, and the Jet Propulsion Laboratory/California Institute of Technology, funded by the National Aeronautics and Space Administration. This research has made (extensive) use of the SIMBAD database, operated at CDS, Strasbourg, France.

ORIGINAL UNEDITED MANUSCRIPT

Downloaded from academic.oup.com/mnras/advance-article/doi/10.1093/mnras/stag1822/8836705 by guest on 28 September 2026

## DATA AVAILABILITY

Photometric IR catalogues from 2MASS, *Spitzer*, *WISE* are available at the NASA/IPAC Infrared Science Archive (IRSA)[6] while SPHEREx spectrophotometry can also be accessed from IRSA[7]

## REFERENCES


Akeson R., et al., 2025, arXiv e-prints, p. arXiv:2511.15823
Arthur S. J., 2025, MNRAS, 543, 1158
Bailer-Jones C. A. L., Rybizki J., Fouesneau M., Demleitner M., Andrae R., 2021, AJ, 161, 147
Benjamin R. A., et al., 2003, PASP, 115, 953
Bernard Salas J., Pottasch S. R., Beintema D. A., Wesselius P. R., 2001, A&A, 367, 949
Bloecker T., 1995, A&A, 299, 755
Bock J. J., et al., 2026, ApJ, 999, 139
Bohannan B., Crowther P. A., 1999, ApJ, 511, 374
Böker T., et al., 2023, PASP, 135, 038001
Bucciarelli B., Stanghellini L., 2023, A&A, 680, A104
Callingham J. R., Tuthill P. G., Pope B. J. S., Williams P. M., Crowther P. A., Edwards M., Norris B., Kedziora-Chudczer L., 2019, Nature Astronomy, 3, 82
Callingham J. R., Crowther P. A., Williams P. M., Tuthill P. G., Han Y., Pope B. J. S., Marcote B., 2020, MNRAS, 495, 3323
Carrasco J. M., et al., 2021, A&A, 652, A86
Chang J., Wang W., Qu M., Su K., Tu L., Lv C., Jiang B., Zhang Y., 2025, ApJS, 280, 10
Chené A.-N., et al., 2013, A&A, 549, A98
Cioni M.-R. L., et al., 2011, A&A, 527, A116
Clark J. S., Najarro F., Negueruela I., Ritchie B. W., Urbaneja M. A., Howarth I. D., 2012, A&A, 541, A145
Creevey O. L., et al., 2023, A&A, 674, A26
Cropper M., et al., 2018, A&A, 616, A5
Crowther P. A., 2007, ARA&A, 45, 177
Crowther P. A., 2015, in Hamann W.-R., Sander A., Todt H., eds, Wolf-Rayet Stars. pp 21–26 (arXiv:1509.00495), doi:10.48550/arXiv.1509.00495
Crowther P. A., Smith L. J., 1999, MNRAS, 308, 82
Crowther P. A., Hillier D. J., Smith L. J., 1995, A&A, 293, 403
Crowther P. A., De Marco O., Barlow M. J., 1998, MNRAS, 296, 367
Crowther P. A., Hadfield L. J., Clark J. S., Negueruela I., Vacca W. D., 2006a, MNRAS, 372, 1407
Crowther P. A., Morris P. W., Smith J. D., 2006b, ApJ, 636, 1033
Crowther P. A., Schnurr O., Hirschi R., Yusof N., Parker R. J., Goodwin S. P., Kassim H. A., 2010, MNRAS, 408, 731
Crowther P. A., Barlow M. J., Royer P., Hillier D. J., Bestenlehner J. M., Morris P. W., Wesson R., 2024, MNRAS, 528, 2026
Davies B., et al., 2012, MNRAS, 419, 1871
De Angeli F., et al., 2023, A&A, 674, A2
De Marco O., Crowther P. A., 1999, MNRAS, 306, 931
Dessart L., Crowther P. A., Hillier D. J., Willis A. J., Morris P. W., van der Hucht K. A., 2000, MNRAS, 315, 407
Drout M. R., Götberg Y., Ludwig B. A., Groh J. H., de Mink S. E., O'Grady A. J. G., Smith N., 2023, Science, 382, 1287
Event Horizon Telescope Collaboration et al., 2022, ApJ, 930, L12
Faherty J. K., Shara M. M., Zurek D., Kanarek G., Moffat A. F. J., 2014, AJ, 147, 115
Figer D. F., McLean I. S., Najarro F., 1997, ApJ, 486, 420
Götberg Y., de Mink S. E., Groh J. H., Kupfer T., Crowther P. A., Zapartas E., Renzo M., 2018, A&A, 615, A78
Götberg Y., et al., 2023, ApJ, 959, 125
Gräfener G., Koesterke L., Hamann W.-R., 2002, A&A, 387, 244
Hadfield L. J., van Dyk S. D., Morris P. W., Smith J. D., Marston A. P., Peterson D. E., 2007, MNRAS, 376, 248
Hamann W.-R., Gräfener G., 2003, A&A, 410, 993
Hamann W.-R., Gräfener G., Liermann A., 2006, A&A, 457, 1015
Hanson M. M., Conti P. S., Rieke M. J., 1996, ApJS, 107, 281
Hillier D. J., Crowther P. A., Najarro F., Fullerton A. W., 1998, A&A, 340, 483
Hobbs D., et al., 2021, Experimental Astronomy, 51, 783
Hopewell E. C., et al., 2005, MNRAS, 363, 857
Houck J. R., et al., 2004, in Mather J. C., ed., Society of Photo-Optical Instrumentation Engineers (SPIE) Conference Series Vol. 5487, Optical, Infrared, and Millimeter Space Telescopes. pp 62–76, doi:10.1117/12.550517
Ignace R., Cassinelli J. P., Tracy G., Churchwell E., Lamers H. J. G. L. M., 2007, ApJ, 669, 600
Indebetouw R., et al., 2005, ApJ, 619, 931
Kanarek G. C., Shara M. M., Faherty J. K., Zurek D., Moffat A. F. J., 2017, MNRAS, 465, 293
Kingsburgh R. L., Barlow M. J., Storey P. J., 1995, A&A, 295, 75
Kollmeier J. A., et al., 2026, AJ, 171, 52
Kudritzki R. P., Urbaneja M. A., Puls J., 2006, in Barlow M. J., Méndez R. H., eds, IAU Symposium Vol. 234, Planetary Nebulae in our Galaxy and Beyond. pp 119–126 (arXiv:astro-ph/0608094), doi:10.1017/S1743921306002857
Lau R. M., et al., 2022, Nature Astronomy, 6, 1308
Lenorzer A., Vandenbussche B., Morris P., de Koter A., Geballe T. R., Waters L. B. F. M., Hony S., Kaper L., 2002, A&A, 384, 473
Maíz Apellániz J., et al., 2016, ApJS, 224, 4
Marin L. C., Massey P., Skiff B. A., Farrell K. A., 2024, AJ, 168, 167
Massey P., Conti P., 1980, ApJ, 242, 638
Mauerhan J. C., Cotera A., Dong H., Morris M. R., Wang Q. D., Stolovy S. R., Lang C., 2010, ApJ, 725, 188
Mauerhan J. C., Van Dyk S. D., Morris P. W., 2011, AJ, 142, 40
Mauerhan J., Smith N., Van Dyk S. D., Morzinski K. M., Close L. M., Hinz P. M., Males J. R., Rodigas T. J., 2015, MNRAS, 450, 2551
McGregor P. J., Hyland A. R., Hillier D. J., 1988, ApJ, 324, 1071
Miller Bertolami M. M., 2016, A&A, 588, A25
Miszalski B., Crowther P. A., De Marco O., Köppen J., Moffat A. F. J., Acker A., Hillwig T. C., 2012, MNRAS, 423, 934
Moffat A. F. J., Breysacher J., Seggewiss W., 1985, ApJ, 292, 511
Morgan D. H., Parker Q. A., Russeil D., 2001, MNRAS, 322, 877
Morris P. W., Eenens P. R. J., Hanson M. M., Conti P. S., Blum R. D., 1996, ApJ, 470, 597
Morris P. W., van der Hucht K. A., Crowther P. A., Hillier D. J., Dessart L., Williams P. M., Willis A. J., 2000, A&A, 353, 624
Morris P. W., Crowther P. A., Houck J. R., 2004, ApJS, 154, 413
Mulato L., Merc J., Charbonnel S., Garde O., Le Du P., Petit T., 2025, A&A, 695, A227
Mulato L., Merc J., Charbonnel S., Garde O., Le Dû P., Petit T., 2026, A&A, 710, A298
Müller-Horn J., et al., 2026, arXiv e-prints, p. arXiv:2608.05276
Najarro F., Hillier D. J., Stahl O., 1997, A&A, 326, 1117
Nishimaki Y., Yamamuro T., Motohara K., Miyata T., Tanaka M., 2008, PASJ, 60, 191
Pauldrach A. W. A., Hoffmann T. L., Méndez R. H., 2004, A&A, 419, 1111
Penoyre Z., Belokurov V., Evans N. W., 2022, MNRAS, 513, 2437
Rate G., Crowther P. A., 2020, MNRAS, 493, 1512
Rate G., Crowther P. A., Parker R. J., 2020, MNRAS, 495, 1209
Romagnolo A., Gormaz-Matamala A. C., Belczynski K., 2024, ApJ, 964, L23
Rosslowe C. K., Crowther P. A., 2015, MNRAS, 447, 2322
Rosslowe C. K., Crowther P. A., 2018, MNRAS, 473, 2853
Sander A. A. C., Vink J. S., 2020, MNRAS, 499, 873
Sander A., Hamann W.-R., Todt H., 2012, A&A, 540, A144
Shara M. M., Moffat A. F. J., Smith L. F., Niemela V. S., Potter M., Lamontagne R., 1999, AJ, 118, 390
Shara M. M., et al., 2009, AJ, 138, 402


[6] https://irsa.ipac.caltech.edu/applications/Gator/
[7] https://irsa.ipac.caltech.edu/applications/spherex/tool-spectrophotometry

ORIGINAL UNEDITED MANUSCRIPT

Downloaded from academic.oup.com/mnras/advance-article/doi/10.1093/mnras/stag1822/8836705 by guest on 28 September 2026

Shara M. M., Faherty J. K., Zurek D., Moffat A. F. J., Gerke J., Doyon R., Artigau E., Drissen L., 2012, AJ, 143, 149
Shenar T., 2026, in Encyclopedia of Astrophysics, Volume 2. pp 569–583 (arXiv:2410.04436), doi:10.1016/B978-0-443-21439-4.00031-6
Shenar T., et al., 2023, Science, 381, 761
Skrutskie M. F., et al., 2006a, AJ, 131, 1163
Skrutskie M. F., et al., 2006b, AJ, 131, 1163
Smith L. J., Crowther P. A., Prinja R. K., 1994, A&A, 281, 833
Smith L. F., Shara M. M., Moffat A. F. J., 1996, MNRAS, 281, 163
Todt H., Hamann W.-R., 2015, in Hamann W.-R., Sander A., Todt H., eds, Wolf-Rayet Stars. pp 253–258
Tramper F., et al., 2015, A&A, 581, A110
Verstraete L., et al., 2001, A&A, 372, 981
Weidmann W. A., et al., 2020, A&A, 640, A10
Werner K., Todt H., Bond H. E., Zeimann G. R., 2024, A&A, 686, A29
Williams P. M., 2019, MNRAS, 488, 1282
Wright E. L., et al., 2010, AJ, 140, 1868
van der Hucht K. A., 2001, New Astron. Rev., 45, 135
van der Hucht K. A., et al., 1996, A&A, 315, L193

## APPENDIX A: SPHEREX SPECTROPHOTOMETRY OF ADDITIONAL SOURCES

Figure A1 presents SPHEREx spectrophotometry of the Planetary Nebula NGC 2392, [WC4]-type central star PMR 1 (Morgan et al. 2001), WC8 star WR123-4 a.k.a. 1603-75L from Shara et al. (2012), plus newly identified sources G31.2-1.3 [WC7-8] G307.2-0.6 [WC8-9], G326.5-0.6 [WC9] together with photometry from 2MASS (open circles), *Spitzer*/ GLIMPSE (open squares) and *WISE* (open triangles). Nebular emission dominates the 1–5$\mu$m spectrum of NGC 2392, whereas stellar wind He II and C IV lines dominate the spectrum of PMR 1, with C IV 2.08$\mu$m weak, as in the [WO]-type central star NGC 6905 and [WC]-type central star NGC 6751 (Fig. 2). WR123-4 exhibits the blend of C IV 2.08$\mu$m with C III 2.11$\mu$m, but suffers from high dust extinction, with J$\sim$16.7 mag. The candidate CSPNe host late spectral type central stars, so also include C III 0.97$\mu$m, with C IV 2.08$\mu$m prominent in G31.2-1.3 and G307.2-0.6.

Figure A2 presents SPHEREx spectrophotometry of the He II emission line sources J1823+0250 and J1907-0523, and the recently identified WN binary WR2-1 (Müller-Horn et al. 2026), together with photometry from 2MASS (open circles) and *WISE* (open triangles). J1823+0250 and J1907-0523 both show He II 1.01$\mu$m, 1.86$\mu$m, 3.09$\mu$m, 4.76$\mu$m, with He I 1.08$\mu$m also observed in J1823+0250. The higher resolving power of SPHEREx in Band B6 perhaps an assessment of stellar vs nebular origin of He II 4.76$\mu$m. This is consistent with a nebular in origin for J1823+0250, whereas J1907-0523 is significantly broadened, suggesting a stellar origin. WR2-1 reveals prominent He II 3.09$\mu$m and 4.76$\mu$m, plus P$\alpha$+He II and Br$\alpha$+He II. Notably, the He II 4.76$\mu$m emission in WR2-1 could also be inferred to be nebular in origin owing to its slow wind (Müller-Horn et al. 2026).

ORIGINAL UNEDITED MANUSCRIPT

Downloaded from academic.oup.com/mnras/advance-article/doi/10.1093/mnras/stag1822/8836705 by guest on 28 September 2026

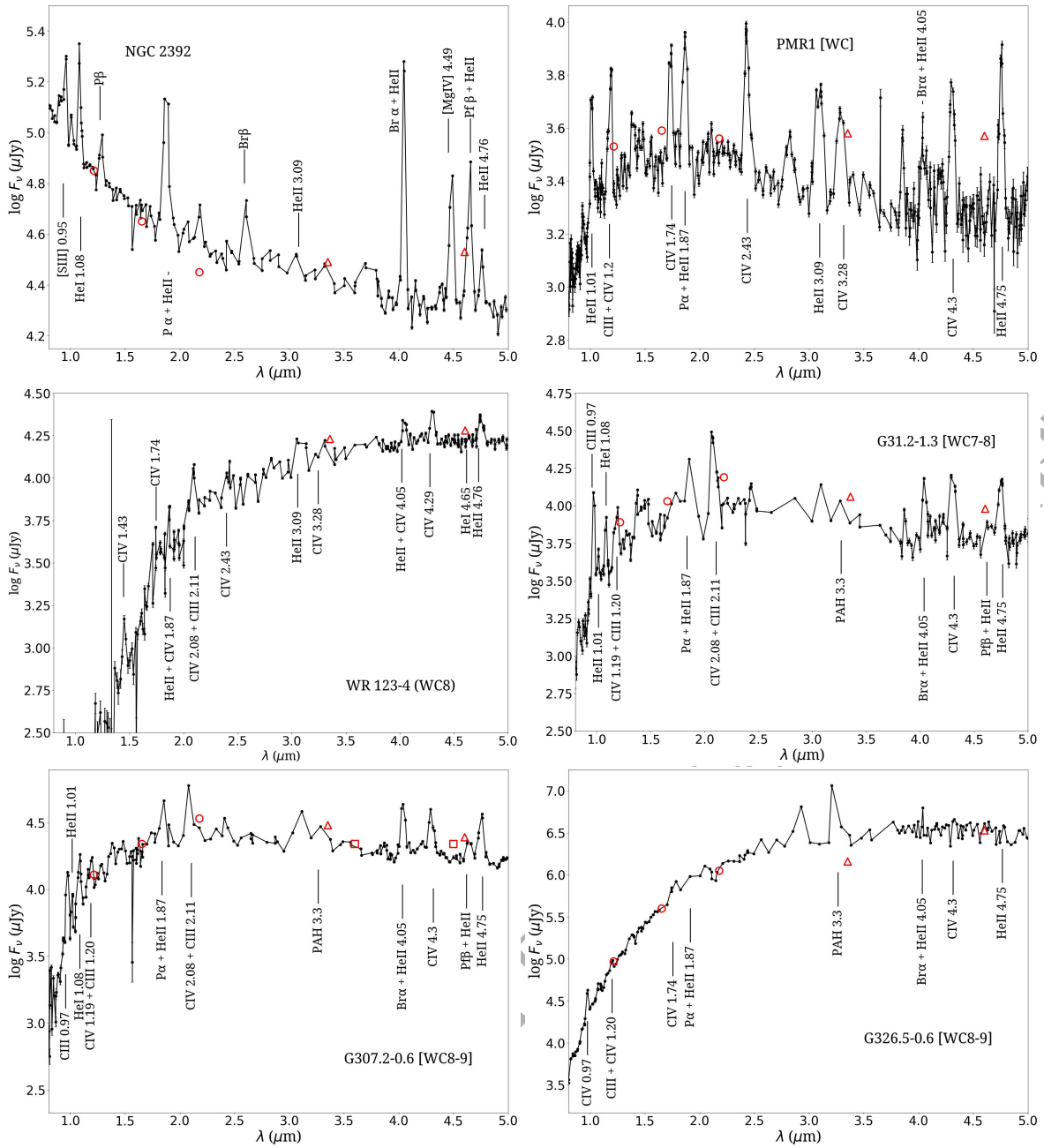



**Figure A1.** SPHEREx spectrophotometry of the Planetary Nebula NGC 2392 (top left), [WC]-type central star PMR 1 (top right), WC8 star WR123-4 (middle left) a.k.a. 1603-75L from Shara et al. (2012), plus newly identified sources G31.2-1.3 (middle right), G307.2-0.6 (bottom left) and G326.5-0.6 (bottom right) together with photometry from 2MASS (open circles), *Spitzer*/GLIMPSE (open squares) and *WISE* (open triangles). Spectrophotometry of WR123-4 infers near-IR photometry of J~16.7 mag, H~14.3 mag and K~12.4, contrary to the 2MASS source 11″ to its north with K=13.68 mag quoted by Shara et al. (2012).

ORIGINAL UNEDITED MANUSCRIPT

Downloaded from academic.oup.com/mnras/advance-article/doi/10.1093/mnras/stag1822/8836705 by guest on 28 September 2026

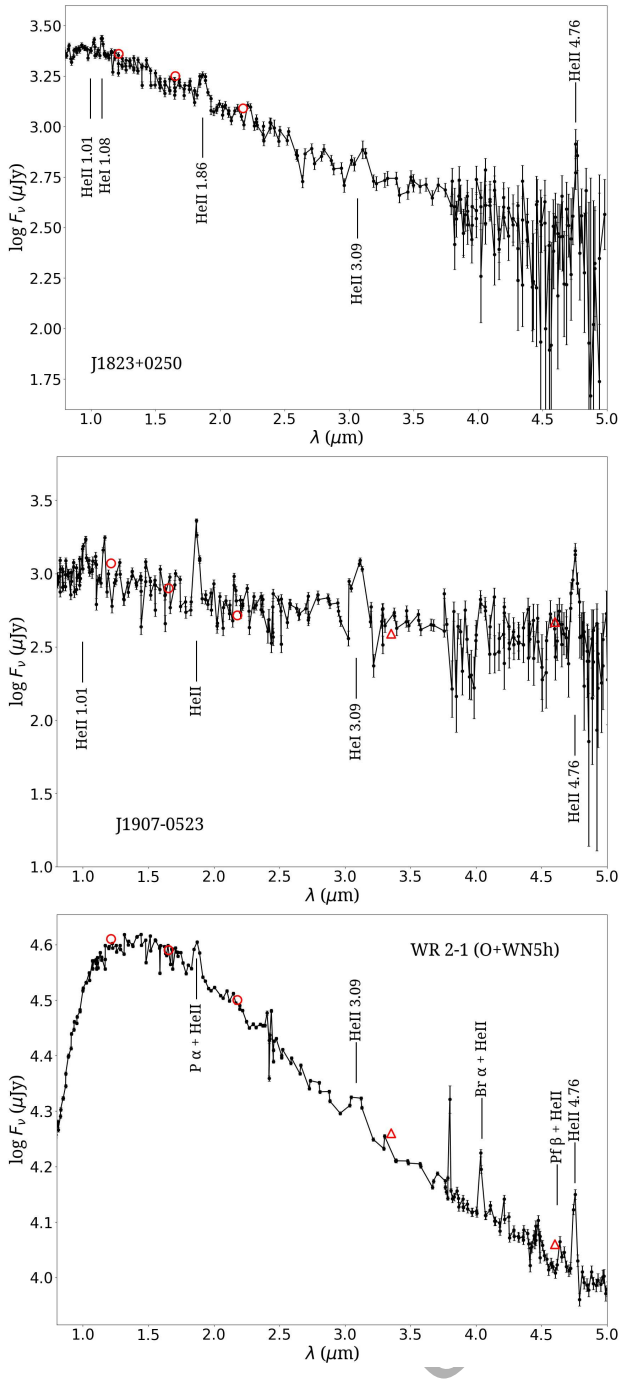



**Figure A2.** SPHEREx spectrophotometry of the He II emission line sources J1823+0250 (top) and J1907-0523 (middle), plus the newly identified O+WN system WR2-1 from Müller-Horn et al. (2026, bottom), together with photometry from 2MASS (open circles) and *WISE* (open triangles).

ORIGINAL UNCITED MANUSCRIPT

Downloaded from academic.oup.com/mnras/advance-article/doi/10.1093/mnras/stag1822/8836705 by guest on 28 September 2026